GEOPHYSICAL RESEARCH LETTERS, VOL. 26, NO. 7, PAGES 843-846, APRIL 1, 1999

Simulation of the $k^{-5/3}$ mesoscale spectral regime in the GFDL SKYHI general circulation model

John N. Koshyk

Department of Physics, University of Toronto, Toronto, Ontario, Canada

Kevin Hamilton and J. D. Mahlman

Geophysical Fluid Dynamics Laboratory/NOAA, Princeton, New Jersey

Abstract. Data from very high horizontal resolution simulations with the Geophysical Fluid Dynamics Laboratory SKYHI general circulation model are used to calculate the kinetic energy spectrum as a function of horizontal wavenumber, k, in the upper troposphere. The spectrum shows the familiar $\sim$ -3 slope at scales longer than $\sim$ 1000 km, in agreement with previous general circulation model and observational studies. At shorter scales, the spectrum becomes shallower with a slope $\sim$ -5/3, also in agreement with available observations. The -5/3 slope spans about a decade of the resolved scales and this result represents the first successful simulation of such a broad range of the mesoscale regime by a global model. Partitioning of the flow between rotational and divergent components shows that the rotational part dominates at large scales and that there is approximate equipartition between rotational and divergent parts at mesoscales. Analysis of the parameterized kinetic energy dissipation shows that vertical diffusion dominates horizontal diffusion for a wide range of wavenumbers extending well into the $k^{-5/3}$ regime.

1. Introduction

It is well established that the horizontal kinetic energy (KE) spectrum in the free troposphere for wavelengths longer than $\sim$ 1000 km follows a $\sim k^{-3}$ power law where k is the horizontal wavenumber [*Baer*, 1972; *Boer and Shepherd*, 1983; *Chen and Wiin-Neilsen*, 1978; *Koshyk and Boer*, 1995]. This is in agreement with the prediction of two-dimensional turbulence theory for a downscale enstrophy-cascading inertial subrange [*Batchelor*, 1969; *Kraichnan*, 1967] and, more generally, with the theory of geostrophic turbulence [*Charney*, 1971].

For horizontal wavelengths smaller than $\sim$ 1000 km (the atmospheric mesoscale), analyses of observed data from various sources have shown that the horizontal KE spectrum follows a $\sim k^{-5/3}$ power law [*Gage*, 1979; *Nastrom et al.*, 1984]. *Nastrom et al.* [1984] analyzed detailed wind observations in the upper troposphere from instrumented commercial aircraft. A summary of data from several thousand flights is shown by the data points on Figure 1, where power spectra of the zonal wind, u, and the meridional wind, v, are displayed separately. The straight lines shown for reference have slopes of -3 and -5/3. There is a fairly well-defined break in the spectra at wavelengths of $\sim$ 500-1000 km with shallower spectral slopes of $\sim$ -5/3 at smaller scales.

While there is reasonably convincing theory for the $\sim k^{-3}$ spectral range at large spatial scales, the explanation for the relatively shallow spectrum in the mesoscale is less clear. One hypothesis is that the $k^{-5/3}$ regime is a two-dimensional inertial subrange in which KE cascades upscale from a relatively small scale source associated with moist convective processses [*Gage*, 1979]. The results of certain modelling studies support this view [*Lilly*, 1969, 1983; *Vallis et al.*, 1997]. A competing hypothesis suggests that motions in the $k^{-5/3}$ regime are neither purely two-dimensional nor balanced (i.e. characterized by low Rossby and Froude numbers) but contain a significant divergent component associated with internal gravity waves [*VanZandt*, 1982]. A number of modelling studies have shown that, when fully divergent motions are allowed, a large-scale KE source can force a flow that spontaneously produces smaller scale gravity waves, in addition to a downscale cascade of enstrophy [*Bartello*, 1995; *Farge and Sadourny*, 1989; *Polvani et al.*, 1994; *Yuan and Hamilton*, 1994].

Atmospheric general circulation models (GCMs) have successfully simulated a realistic $\sim k^{-3}$ regime [*Charney*, 1971; *Boer et al.*, 1984; *Koshyk and Boer*, 1995; *Laursen and Eliasen*, 1989] but the horizontal resolution of such models is typically too coarse to explicitly resolve atmospheric mesoscales. The present note describes the first realistic simulation of the upper tropospheric KE spectrum in an unprecedentedly high resolution atmospheric GCM.

2. Description of the model

The model employed is the Geophysical Fluid Dynamics Laboratory (GFDL) SKYHI GCM that solves the governing equations discretized on a global latitude-longitude grid [*Hamilton et al.*, 1995]. Results are described from versions of the model with 1° x 1.2° and 0.33° x 0.40° horizontal resolution (denoted N90 and N270 respectively, where the notation refers to the number of latitude rows in one hemisphere), and either 40 (L40) or 80 (L80) levels in the vertical between the ground and $\sim$ 80 km. The vertical resolution in the upper troposphere is $\sim$ 1 km at L40 and $\sim$ 500 m at L80. Some realistic mesoscale structures have been found in preliminary examinations of the tropospheric simulation with the N270 model [*Hamilton and Hemler*, 1997]. In addition, horizontal spectra of N_2O in the lower stratosphere have been computed from N90L40 data [*Strahan and Mahlman*, 1994*a,b*] and agree well with comparably sampled data from lower stratospheric research flights.

Paper number 1999GL900128.
0094-8276/99/1999GL900128$05.00

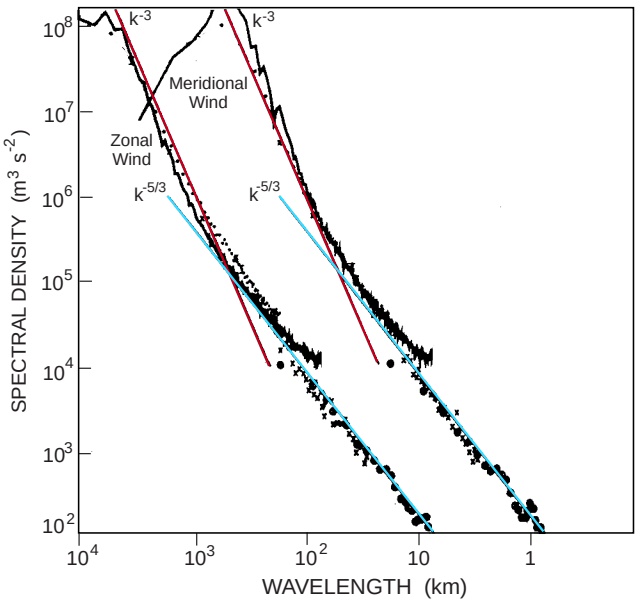

Figure 1. One-dimensional horizontal Fourier power spectra of the zonal and meridional wind components in the upper troposphere. The data points are reproduced from *Nastrom et al.* [1984] and show actual observations based on data from commercial aircraft flights, with different symbols representing results obtained using different lengths of flight segments. The straight lines are drawn for reference and have slopes of -5/3 and -3. The solid curve is for the 0.33° x 0.40° x 40-levels (N270L40) SKYHI model along the 45°N latitude circle, monthly averaged for a single July. For clarity the results for the meridional wind have been shifted one decade to the right.

In common with other GCMs, the SKYHI model includes parameterizations of both vertical and horizontal subgrid-scale dynamical effects in the horizontal momentum equations. The vertical momentum mixing is treated as a second-order diffusion with coefficient, K_V, that varies as a function of the model level spacing and the local Richardson number, Ri, of the resolved flow as follows:

$$\begin{aligned} K_V &= 0 && \text{if } Ri > A/4, \\ &= l^2\, S(1-4Ri/A)^{1/2} && \text{if } 0 < Ri < A/4, \\ &= l^2\, S && \text{if } Ri < 0, \end{aligned} \qquad (1)$$

where the mixing length $l = 30$ m, S is the magnitude of the vertical wind shear and $A = 1+0.1(\Delta z/100)^{3/2}$, where Δz is the vertical grid spacing in m [*Levy et al.*, 1982]. The factor A provides a statistical correction for the Ri overestimate when $\Delta z \gg 100$ m, the typical scale of turbulent layers in the atmosphere.

The horizontal subgrid-scale mixing is based on the nonlinear eddy viscosity scheme of *Smagorinsky* [1963]. The nonlinear diffusion coefficient is given by $K_H = (k_\circ \Delta y)^2 |D|$ where $k_\circ = 0.1$ is a dimensionless constant, Δy is the horizontal grid spacing, and $|D|$ is the magnitude of the horizontal flow deformation [*Andrews et al.*, 1983]. This formulation arises from a similarity argument that yields a quasi-two-dimensional analog of Kolmogoroff's three-dimensional inertial turbulence range. In effect, the assumption is made that irreversible mixing occurs when the fluid undergoes significant horizontal deformation-induced strain.

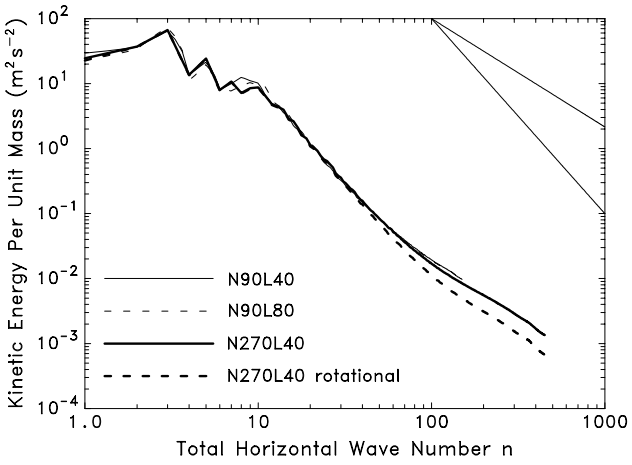

Figure 2. July mean total kinetic energy spectra as functions of total spherical harmonic wavenumber n, calculated from the SKYHI model. The nondimensional value $n = 1$ corresponds to a wavelength $\sim$ 40,000 km. The curves represent vertically-averaged values over the 104-320 mb layer for resolutions: N90L40, N90L80 and N270L40 (see text for description). The N270L40 spectrum calculated using the rotational part of the wind only is also shown. Straight lines in the upper right-hand corner have slopes of -5/3 and -3.

The version of the model used here has no parameterization of subgrid-scale gravity-wave momentum fluxes. However, gravity waves in the model are spontaneously generated by a variety of mechanisms including flow over topography and moist convection. The moist convection contribution has been characterized in lower resolution versions of the model, and shown to be very important [*Manzini and Hamilton*, 1993]. SKYHI is formulated with a time-marching scheme that allows explicit representation of short-period gravity waves, in distinction to many other GCMs in which high-frequency motions are deliberately suppressed.

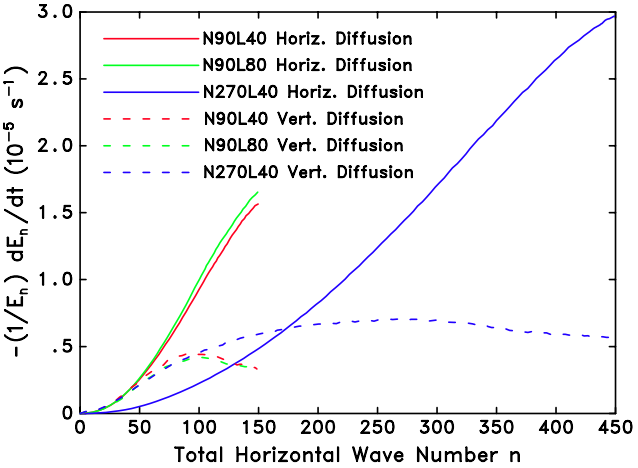

Figure 3. Normalized dissipation rates for kinetic energy due to parameterized subgrid-scale diffusion of momentum in the three SKYHI simulations, temporally averaged over July and vertically-averaged over the 104-320 mb layer. Results are shown separately for the horizontal diffusion and the vertical diffusion.

3. Results and discussion

The thick solid curves in Figure 1 show Fourier spectra of u and v around the 45°N latitude circle at 211 mb in the N270L40 run, averaged over 1488 half-hourly snapshots for a single July. These results can be appropriately compared with the commercial aircraft observations shown in Figure 1, taken primarily from levels near 200 mb during midlatitude trans-Atlantic or trans-Pacific flights. The agreement between the model and observations is quite good, although there is some disagreement at the very smallest scales, where the model spectra have higher values of KE than the observations. Both the model and observations show steep slopes at large scales and significantly shallower slopes at mesoscales. The model Fourier spectra vary with latitude, with generally shallower slopes at tropical latitudes (not shown) compared to extratropical latitudes.

The horizontal KE spectrum per unit mass as a function of total spherical harmonic wavenumber, n, can also be computed from spectral coefficients for vorticity, ζ_n^m, and divergence, δ_n^m, as follows:

$$E_n^m(p,t) = \frac{1}{4}\frac{a^2}{[n(n+1)]}(|\zeta_n^m|^2 + |\delta_n^m|^2) \qquad (2)$$

where a is Earth's radius and m is the zonal wavenumber [*Lambert*, 1984]. Alternatively, E_n^m can be written directly in terms of horizontal velocity coefficients u_n^m and v_n^m [*Baer*, 1972]. However, (2) has the attractive property that the contributions to the KE from the rotational and divergent parts of the flow can easily be separated. Differences between velocity-based spectra (not shown here) and those obtained from (2) decrease rapidly with wavenumber, and are negligible beyond the largest decade of spatial scales.

Mean KE spectra for a single July derived from the N90L40, N90L80 and N270L40 simulations as functions of n are shown in Figure 2, vertically averaged between 320 and 104 mb. A sum over the zonal wavenumber m has been performed for each value of n. The N90 and N270 expansions are truncated at $n = 150$ and 450 respectively, where $n = 1$ corresponds to a horizontal wavelength of $\sim$ 40,000 km. The N90L40 and N90L80 spectra are almost identical at all wavenumbers, indicating numerical convergence with vertical resolution for this aspect of the simulations. The N270 and N90 results also agree quite well up to $n \sim 80$, suggesting that over a very wide range of scales these particular statistical properties of the model simulations have converged. Results for January are very similar to those for July, differing significantly only at planetary scales. The vertical variation in model spectra between 320 and 104 mb is modest, with lower stratospheric spectral amplitudes weaker and slopes shallower than in the upper troposphere for $n \gtrsim 10$.

Near $n \sim 100$ the N270 result in Figure 3 displays a clear break in spectral slope from $\sim$ -3 to $\sim$ -5/3. The -5/3 range is evident well upscale of the wavenumber corresponding to $4\Delta x$, or $n \approx 225$, where Δx is the horizontal grid spacing, so is clearly not a numerical artifact of the model. A shallower slope regime is also evident in the N90 curves over about the highest 50 resolved wavenumbers. The N270 KE spectrum calculated from (2) using the rotational part of the flow only is also shown. Rotational and divergent motions make approximately equal contributions to the KE for $n \gtrsim 100$.

Figure 3 shows the KE dissipation rates for the horizontal and vertical subgrid-scale mixing parameterizations, normalized by the KE spectrum itself. In both the N90 models the energy dissipation from the horizontal diffusion dominates that from the vertical diffusion except at very small wavenumbers. In the N270 simulation, the dissipation from vertical diffusion clearly dominates over the first $\sim$ 150 wavenumbers, since the horizontal diffusion is drastically reduced compared to N90 values. The vertical diffusion rates are much less sensitive to the vertical resolution (changing little between the N90L40 and N90L80 simulations) than the horizontal diffusion rates are to the horizontal resolution (c.f. the N90 and N270 simulations). Thus, it may be anticipated that with increases in both horizontal and vertical resolution beyond N270L40, vertical diffusion will be the limiting dissipative process over the $\sim$ -3 and much of the $\sim$ -5/3 spectral ranges, leaving the spectrum largely insensitive to details of the horizontal diffusion parameterization.

4. Conclusions

An unprecedentedly high resolution version of the GFDL SKYHI GCM has been used to realistically simulate the observed $k^{-5/3}$ mesoscale KE spectrum. The presence of a strong divergent component in the $k^{-5/3}$ regime suggests that this range is likely not well approximated by a two-dimensional inertial subrange, nor is it characterized by the type of low Froude number balance discussed, for example, in *Lilly*, [1983]. It does, however, suggest an important role for gravity waves in this spectral range [*VanZandt*, 1982]. The sources and sinks of these waves, as well as the nature of spectral interactions among different wavenumber components is a subject of current study. Comparison of the parameterized horizontal and vertical mixing processes among model versions with various resolutions showed that vertical mixing processes dominate over an increasingly broad wavenumber band as resolution is increased. Further analysis will focus on the available potential energy and vertical velocity spectra in the model, on the detailed dynamics maintaining the simulated mesoscale spectrum and on the spectral dynamics at levels in the stratosphere and mesosphere.

Acknowledgments. The authors are grateful to Prof. T. G. Shepherd, Dr. G. K. Vallis and two anonymous reviewers for their helpful comments and to R. Hemler and R. J. Wilson for their assistance with the model integrations. Greg Nastrom kindly granted permission to reproduce the observational data in Figure 1.

References

Andrews, D. G., J. D. Mahlman, and R. W. Sinclair, Eliassen-Palm diagnostics of wave-mean flow interactions in the GFDL SKYHI general circulation model, *J. Atmos. Sci.*, *40*, 2768-2784, 1972.

Baer, F., An alternate scale representation of atmospheric energy spectra, *J. Atmos. Sci.*, *29*, 649-664, 1972.

Bartello, P., Geostrophic adjustment and inverse cascades in rotating stratified turbulence, *J. Atmos. Sci.*, *52*, 4410-4428, 1995.

Batchelor, G. K., Computation of the energy spectrum in homogeneous two-dimensional turbulence, *Phys. Fluids Suppl. II*, *12*, 233-239, 1969.

Boer, G. J., and T. G. Shepherd, Large-scale two-dimensional turbulence in the atmosphere, *J. Atmos. Sci.*, *40*, 164-184, 1983.

Boer, G. J., N. A. McFarlane, and R. Laprise, The climatology of the Canadian Climate Centre general circulation model as obtained from a five-year simulation, *Atmos.-Ocean*, *22*, 430-473, 1984.

Charney, J. G., Geostrophic turbulence, *J. Atmos. Sci.*, *28*, 1087-1095, 1971.

Chen, T.-C., and A. Wiin-Nielsen, Non-linear cascades of atmospheric energy and enstrophy in a two-dimensional spectral index, *Tellus*, *30*, 313-322, 1978.

Farge, M., and R. Sadourny, Wave-vortex dynamics in rotating shallow water, *J. Fluid Mech.*, *206*, 443-462, 1989.

Gage, K. S., Evidence for a $k^{-5/3}$ power law inertial range in mesoscale two-dimensional turbulence, *J. Atmos. Sci.*, *36*, 1950-1954, 1979.

Hamilton, K., R. J. Wilson, J. D. Mahlman, and L. J. Umscheid, Climatology of the SKYHI troposphere-stratosphere-mesosphere general circulation model, *J. Atmos. Sci.*, *52*, 5-43, 1995.

Hamilton, K., and R. S. Hemler, Appearance of a supertyphoon in a global climate model simulation, *Bull. Am. Meteorol. Soc., 78*, 2874-2876, 1997.

Koshyk, J. N., and G. J. Boer, Parameterization of dynamical subgrid-scale processes in a spectral GCM, *J. Atmos. Sci.*, *52*, 965-976, 1995.

Kraichnan, R., Inertial ranges in two-dimensional turbulence, *Phys. Fluids*, *10*, 1417-1423, 1967.

Lambert, S. J., A global available potential energy-kinetic energy budget in terms of the two-dimensional wavenumber for the FGGE year, *Atmos.-Ocean*, *22*, 265-282, 1984.

Levy, H., J. D. Mahlman, and W. J. Moxim, Tropospheric N_2O variability, *J. Geophys. Res., 87*, 3061-3080, 1982.

Lilly, D. K., Numerical simulation of two-dimensional turbulence, *Phys. Fluids Suppl. II*, *12*, 240-249, 1969.

Lilly, D. K., Stratified turbulence and the mesoscale variability of the atmosphere, *J. Atmos. Sci.*, *40*, 749-761, 1983.

Laursen, L., and E. Eliasen, On the effects of the damping mechanisms in an atmospheric general circulation model, *Tellus*, *41A*, 385-400, 1989.

Manzini, E., and K. Hamilton, Middle atmosphere traveling waves forced by latent and convective heating, *J. Atmos. Sci.*, *50*, 2180-2200, 1993.

Nastrom, G. D., K. S. Gage, and W. H. Jasperson, Kinetic energy spectrum of large- and mesoscale atmospheric processes, *Nature*, *310*, 36-38, 1984.

Polvani, L. M., J. C. McWilliams, M. A. Spall, and R. Ford, The coherent structures of shallow water turbulence: deformation radius effects, cyclone/anticyclone asymmetry and gravity-wave generation, *Chaos*, *4*, 177-186, 1994.

Smagorinsky, J., General circulation experiments with the primitive equations. I. The basic experiment, *Mon. Weather Rev., 94*, 99-164, 1963.

Strahan, S. E., and J. D. Mahlman, Evaluation of the SKYHI general circulation model using aircraft N_2O measurements 1. Polar winter stratospheric meteorology and tracer morphology, *J. Geophys. Res., 99*, 10305-10318, 1994a.

Strahan, S. E., and J. D. Mahlman, Evaluation of the SKYHI general circulation model using aircraft N_2O measurements 2. Tracer variability and diabatic meridional circulation, *J. Geophys. Res., 99*, 10319-10332, 1994b.

Vallis, G. K., G. J. Shutts, and M. E. B. Gray, Balanced mesoscale motion and stratified turbulence forced by convection, *Q. J. R. Meteorol. Soc., 123*, 1621-1652, 1997.

Yuan, L. and K. Hamilton, Equilibrium dynamics in a forced-dissipative f-plane shallow water model, *J. Fluid. Mech.*, *280*, 369-394, 1994.

VanZandt, T. E., A universal spectrum of buoyancy waves in the atmosphere, *Geophys. Res. Lett., 9*, 575-578, 1982.

J. N. Koshyk, Department of Physics, University of Toronto, Toronto, ON, M5S 1A7, Canada. (e-mail:koshyk@mam.physics.utoronto.ca)

K. Hamilton, and J. D. Mahlman, Geophysical Fluid Dynamics Laboratory/NOAA, Princeton University, Princeton, NJ 08542. (e-mail: kph@gfdl.gov; jm@gfdl.gov)

(Received December 17, 1998; revised January 25, 1999; accepted February 16, 1999.)